Lateral chirality-sorting optical forces

Amaury Hayat[a,b,1], J. P. Balthasar Mueller[a,1,2], and Federico Capasso[a,2]

[a]School of Engineering and Applied Sciences, Harvard University, Cambridge, MA 02138; and [b]École Polytechnique, Palaiseau 91120, France

Contributed by Federico Capasso, August 31, 2015 (sent for review June 7, 2015)

The transverse component of the spin angular momentum of evanescent waves gives rise to lateral optical forces on chiral particles, which have the unusual property of acting in a direction in which there is neither a field gradient nor wave propagation. Because their direction and strength depends on the chiral polarizability of the particle, they act as chirality-sorting and may offer a mechanism for passive chirality spectroscopy. The absolute strength of the forces also substantially exceeds that of other recently predicted sideways optical forces.

optical forces | chirality | optical spin-momentum locking | optical spin–orbit interaction | optical spin

Chirality [from Greek $\chi\epsilon\iota\rho$ (*kheir*), "hand"] is a type of asymmetry where an object is geometrically distinct from its mirror image, no matter how it is held or rotated (1). Such objects abound in nature, human hands being the classic example. Even though they share all properties other than their helicity, a chiral object and its mirror image differ in their interaction with chiral environments, such as, for example, biological systems. Analyzing and separating substances by chirality consequently represents an important problem in research and industry, affecting especially pharmaceuticals and agrochemicals (2–5). Whereas the sorting of substances by chirality normally has to be addressed through the introduction of a specific chiral resolving agent (6, 7), the manifestation of chirality in the electromagnetic response of materials has raised the question of passive sorting using optical forces (10–16). In ref. 16 Wang and Chan recently predicted an electromagnetic plane wave to exert a lateral optical force on a chiral particle above a reflective surface, which emerges as the particle interacts with the reflection of its scattered field. This highly unusual force acts in a direction in which there is neither wave propagation nor an intensity gradient, and deflects particles with opposite helicities toward opposite sides. Apart from its fundamental interest, such a force may in theory be useful for all-optical enantiomer sorting with a single, unstructured beam. In ref. 17, Bliokh et al. almost simultaneously predicted another lateral force that is exerted on nonchiral particles in an evanescent wave. This force is a consequence of the linear momentum of the wave that is associated with its extraordinary spin angular momentum (SAM), which was first described by F. J. Belifante in the context of quantum field theory, and which vanishes for a propagating plane wave (18, 19).

In this paper we show that lateral forces can be achieved using a third mechanism, which is also inherently chirality-sorting. The forces emerge through a direct interaction of the optical SAM with chiral particles, and push either in the direction of the SAM vector or opposite to it, depending on the helicity of the particle. In general, the strength and direction of optical SAM may be estimated by considering that SAM manifests itself as a helical polarization of the electromagnetic field. For example, the SAM density of a right-circularly polarized plane wave points in the direction of propagation, and the SAM density of a left-circularly polarized wave in the direction opposite to the direction of propagation. Among plane waves, a circularly polarized wave has the highest optical SAM density, whereas a linearly polarized wave carries none. Elliptically polarized waves represent intermediate cases between these two extremes—the mathematical expression for the optical SAM density of an electromagnetic wave can be found in *Supporting Information*. The optical forces arising through the interaction of light with chiral matter may be intuited by considering that an electromagnetic wave with helical polarization will induce corresponding helical dipole (and multipole) moments in a scatterer. If the scatterer is chiral (one may picture a subwavelength metal helix), then the strength of the induced moments depends on the matching of the helicity of the electromagnetic wave to the helicity of the scatterer. The forces described in this paper, as well as other chirality-sorting optical forces, emerge because the induced moments in the scatterer result in radiation in a helicity-dependent preferred direction, which causes corresponding recoil.

The effect discussed in this paper enables the tailoring of chirality-sorting optical forces by engineering the local SAM density of optical fields, such that fields with transverse SAM can be used to achieve lateral forces. Fields with transverse SAM arise, for example, when light is totally internally reflected at an interface (20–22). Fig. 1, *Inset* shows how totally internally reflected transverse-electric (TE) or transverse-magnetic (TM) polarized waves give rise to evanescent waves with elliptically polarized magnetic and electric fields, respectively. The polarization ellipses of the latter lie in the plane of incidence, implying optical SAM transverse to the direction of wave propagation.

We investigate the lateral chirality-sorting forces by calculating the forces on a small chiral particle in an evanescent field and show that the magnitude of the lateral component of the force substantially exceeds those of the previously predicted lateral forces. To this end, we discuss the optical forces exerted by an electromagnetic wave on a small chiral particle in general and then treat the specific case of an evanescent wave. We then use a nanosphere made of a chiral material to model a small chiral particle and compare the emerging lateral force to the strength of the lateral force that may arise due to the other two effects discussed by Wang and Chan (16) and Bliokh et al. (17). The

Significance

In light of the difficulty often associated with sorting and characterizing materials by chirality, new research aimed toward the development of passive optical methods has stirred considerable excitement at the interface of analytical chemistry and physical optics. We describe here a mechanism through which chirality-sorting optical forces emerge through the interaction with the spin-angular momentum of light, a property that the community has recently learned to control with great sophistication using modern nanophotonics. In particular, the forces may be oriented perpendicularly to the propagation direction of evanescent waves, leading to a helicity-dependent lateral deflection of chiral particles in opposite directions. The highly unusual transverse optical force described herein is the strongest of its kind discovered so far to our knowledge.

Author contributions: A.H., J.P.B.M., and F.C. designed research; A.H. and J.P.B.M. performed research; A.H. and J.P.B.M. analyzed data; and A.H., J.P.B.M., and F.C. wrote the paper.

The authors declare no conflict of interest.

[1]A.H. and J.P.B.M. contributed equally to this work.

[2]To whom correspondence may be addressed. Email: jpbm@seas.harvard.edu or capasso@seas.harvard.edu.

This article contains supporting information online at www.pnas.org/lookup/suppl/doi:10.1073/pnas.1516704112/-/DCSupplemental.

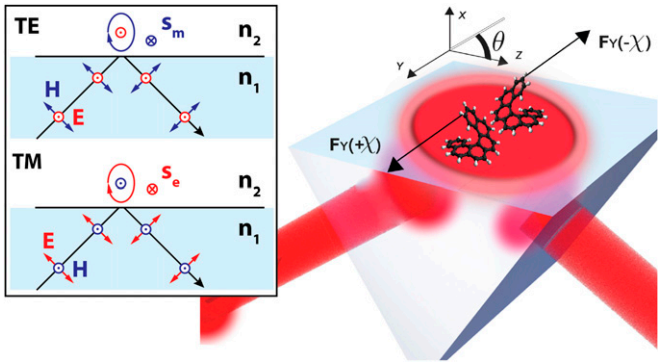

Fig. 1. Chirality-dependent lateral forces in an evanescent field. An evanescent field arises as light in a high index medium (n_1) is totally internally reflected at the interface with a low index medium (n_2) at an angle θ beyond the critical angle. Particles in an evanescent field with transverse spin angular momentum experience lateral forces depending on their chiral polarizability χ, with particles with opposite helicities experiencing lateral forces in oppose directions. (*Inset*) Totally internally reflected TE and TM waves give rise to evanescent waves that have transverse spin due to their elliptically polarized magnetic (TE) and electric (TM) fields.

optical forces exerted on an object are rigorously calculated by first finding the distribution of electromagnetic fields, and then integrating the Maxwell stress tensor over a surface enclosing the object (23). The scattering problem associated with finding the field distributions is tremendously simplified in the dipole approximation, which holds in the so-called Rayleigh limit that applies to particles much smaller than the wavelength. The dipole solution is sufficiently accurate for most molecular scattering problems and is furthermore the basis for efficient numerical methods that are used to find solutions for complex larger objects (24). We consider the optical forces on a small particle in a source-free, lossless, nondispersive, and isotropic medium with relative electric permittivity ε and relative magnetic permeability μ. In the dipole approximation, and in the absence of a permanent electric or magnetic dipole moment of the particle, the time-averaged total optical force $\mathbf{F}$ exerted on the particle by a monochromatic electromagnetic wave is given by (25):

$$\mathbf{F}=\underbrace{\frac{1}{2}\mathrm{Re}\{\mathbf{d}(\nabla\otimes\mathbf{E}^*)+\mathbf{m}(\nabla\otimes\mathbf{H}^*)\}}_{\mathbf{F_0}} \underbrace{-\frac{k^4}{3}\mathrm{Re}\left\{\sqrt{\frac{1}{\mu\epsilon}}(\mathbf{d}\times\mathbf{m}^*)\right\}}_{\mathbf{F_{int}}}, \quad [1]$$

where $\mathbf{E}$ and $\mathbf{H}$ are the electric and magnetic field vectors of the incident electromagnetic wave at the location of the particle, $\mathbf{d}$ and $\mathbf{m}$ are the electric and magnetic dipole moments of the particle that are induced by the incident field, $k=n\omega/c$ is the wavenumber of the electromagnetic wave, ω is the frequency, c is the speed of light in vacuum, and $n=\sqrt{\epsilon\mu}$ is the refractive index of the medium surrounding the dipole. The fields are written in complex phasor notation throughout this paper, where the factor $\exp(-i\omega t)$ giving the time dependence is implied, and the superscript asterisk denotes the complex conjugate. Vector quantities are indicated by bold letters, and all expressions are given in Gaussian units unless stated otherwise. $\hat{\mathbf{x}}$, $\hat{\mathbf{y}}$, and $\hat{\mathbf{z}}$ are unit vectors along the corresponding coordinate axes. The symbol $\otimes$ denotes the dyadic product, so that the terms of the form $\mathbf{W}(\nabla\otimes\mathbf{V})$ in Eq. **1** have elements $[\mathbf{W}(\nabla\otimes\mathbf{V})]_i=\sum_j W_j\partial_i V_j$ for $i,j\in\{x,y,z\}$ (25) and can be written as $\mathbf{W}(\nabla\otimes\mathbf{V})=(\mathbf{W}\cdot\nabla)\mathbf{V}+\mathbf{W}\times(\nabla\times\mathbf{V})$ in terms of more commonly used vector operators. Eq. **1** shows that the optical force has a component $\mathbf{F_0}$ corresponding to the force exerted by the incident field on the particle's electric and magnetic dipole moments, and a component $\mathbf{F_{int}}$ that results from a direct interaction of the two dipole moments. In case of the evanescent field, it is the $\mathbf{F_{int}}$ term that gives rise to the lateral electromagnetic spin force. Chirality manifests itself in the electromagnetic response of a material through a cross-coupling of the induced electric and magnetic polarizations, such that an electric field also gives rise to a magnetic polarization, and vice versa (26, 27). Assuming isotropic polarizabilities and no permanent dipole moment, the electric and magnetic dipole moments induced by fields incident on a chiral particle are $\mathbf{d}=\alpha_e\mathbf{E}+i\chi\mathbf{H}$ and $\mathbf{m}=\alpha_m\mathbf{H}-i\chi\mathbf{E}$, where α_e and α_m are the electric and magnetic polarizabilities (16). The chiral polarizability of the particle χ captures the chiral nature of the dipole, such that setting $\chi=0$ recovers the case of an achiral dipole. It is worth mentioning that, although the chiral polarizability is an inherently dynamic quantity, the dynamic dipole polarizabilities α_e and α_m differ from the more frequently listed corresponding static polarizabilities $\alpha_e^{(0)}$ and $\alpha_m^{(0)}$ by a radiation correction as $\alpha_e=[1-(i2k^3/3\epsilon)\alpha_e^{(0)}]^{-1}\alpha_e^{(0)}$ and $\alpha_m=[1-(i2k^3/3\mu)\alpha_m^{(0)}]^{-1}\alpha_m^{(0)}$ (28, 29). Although the static polarizability turns out to be sufficiently accurate in the particular case of the small metallic sphere considered in ref. 17, omission of the radiation correction can in general lead to a substantial underestimation of the optical forces (*Supporting Information*). The full expression for the force exerted on a chiral dipole by an electromagnetic field is obtained by inserting the expressions for the electric and magnetic dipole moments into Eq. **1**:

$$\mathbf{F_0}=\underbrace{\frac{1}{g}\left(\epsilon^{-1}\mathrm{Re}\{\alpha_e\}\nabla u_e+\mu^{-1}\mathrm{Re}\{\alpha_m\}\nabla u_m\right)-\frac{\omega}{g}\mathrm{Re}\{\chi\}\nabla h}_{\text{Gradient Force}} +\underbrace{\frac{2\omega}{g}\left(\mu\,\mathrm{Im}\{\alpha_e\}\mathbf{p_e^o}+\epsilon\,\mathrm{Im}\{\alpha_m\}\mathbf{p_m^o}\right)-\frac{c}{g}\mathrm{Im}\{\chi\}\left[\nabla\times\mathbf{p}-2k^2\mathbf{s}\right]}_{\text{Radiation Pressure}} \quad [2]$$

$$\mathbf{F_{int}}=-\frac{2\omega}{g}\frac{k^3}{3}\left(\mathrm{Re}\left\{\alpha_e\alpha_m^*\right\}\mathbf{p}-\mathrm{Im}\left\{\alpha_e\alpha_m^*\right\}\mathbf{p}''+|\chi|^2\mathbf{p}\right) -\frac{2\omega}{g}\frac{2k^4}{3n}\left(\epsilon\mathrm{Re}\left\{\chi\alpha_m^*\right\}\mathbf{s_m}+\mu\mathrm{Re}\left\{\chi\alpha_e^*\right\}\mathbf{s_e}\right). \quad [3]$$

Here we marked the terms corresponding to the familiar gradient force and radiation pressure in the first-order term $\mathbf{F_0}$ (Eq. **2**), both of which are modified when the dipole is chiral (i.e., when $\chi\neq0$). The lateral forces are contained in the $\mathbf{F_{int}}$ term, where an additional force term proportional to k^4 emerges for chiral dipoles (the final term of Eq. **3**). This term shows that the spin momentum density of the field gives rise to a linear momentum transfer on chiral particles, which occurs in opposite directions for opposite signs of χ (i.e., opposite helicities). The prefactor $g=(4\pi)^{-1}$ arises from the use of Gaussian units, $u_e=(g\epsilon/4)|\mathbf{E}|^2$ and $u_m=(g\mu/4)|\mathbf{H}|^2$ are the energy densities of the electric and the magnetic field, and $h=(g/2\omega)\mathrm{Im}\{\mathbf{E}\cdot\mathbf{H}^*\}$ is the time-averaged optical helicity density (17, 18). The time-averaged Poynting momentum density $\mathbf{p}=(g/2c)\mathrm{Re}\{\mathbf{E}\times\mathbf{H}^*\}$ can be decomposed as $\mathbf{p}=\mathbf{p^o}+\mathbf{p^s}$ into a component related to the orbital angular momentum, $\mathbf{p^o}$, and the Belifante momentum $\mathbf{p^s}$ related to the spin momentum density $\mathbf{s}$. These quantities can be individually further separated into their electric and magnetic components, in particular $\mathbf{p^o}=\mathbf{p_e^o}+\mathbf{p_m^o}$ and $\mathbf{s}=\mathbf{s_e}+\mathbf{s_m}$ (*Supporting Information* contains a full list of the definitions of the field quantities, which are discussed in detail in ref. 17). Invoking a fluid mechanics analogy, the term $\nabla\times\mathbf{p}$ may be interpreted as the

PHYSICS

vorticity of the Poynting momentum density. $\boldsymbol{p}'' = (g/2c)\mathrm{Im}\{\mathbf{E}\times\mathbf{H}^*\}$ is the imaginary Poynting momentum (17, 30). For a monochromatic wave, the momentum and spin densities are (17):

$$\mathbf{p^s} = -\frac{g}{8\omega}\nabla\times\left[(i\mu)^{-1}\mathbf{E}\times\mathbf{E}^* + (i\epsilon)^{-1}\mathbf{H}\times\mathbf{H}^*\right] \quad \textbf{(4)}$$

$$\mathbf{p^o} = -\frac{g}{4\omega}\mathrm{Im}\left\{\mu^{-1}\mathbf{E}(\nabla\otimes\mathbf{E}^*) + \epsilon^{-1}\mathbf{H}(\nabla\otimes\mathbf{H}^*)\right\} \quad \textbf{[5]}$$

$$\mathbf{s} = -\frac{g}{4\omega}\left((\mu i)^{-1}\mathbf{E}\times\mathbf{E}^* + (\epsilon i)^{-1}\mathbf{H}\times\mathbf{H}^*\right), \quad \textbf{[6]}$$

where the magnetic and electric contributions correspond to the terms proportional to the electric and magnetic fields. Evaluating Eqs. **2** and **3** for a plane wave $\mathbf{E} = \sqrt{\mu}\mathbf{E_0}\exp(ikz)$ propagating in the $\hat{\mathbf{z}}$ direction shows that the forces are entirely in the direction of propagation:

$$\mathbf{F_0} = [(\mathrm{Im}\{\mu\alpha_e\} + \mathrm{Im}\{\epsilon\alpha_m\})/2 + \mathrm{Im}\{\chi\}n\sigma]Ik\ \hat{\mathbf{z}} \quad \textbf{[7]}$$

$$\mathbf{F_{int}} = -\left[\left(\epsilon\,\mathrm{Re}\{\chi\alpha_m^*\} + \mu\,\mathrm{Re}\{\chi\alpha_e^*\}\right)\sigma/n + \mathrm{Re}\{\alpha_e\alpha_m^*\} + |\chi|^2\right]Ik^4/3\ \hat{\mathbf{z}}, \quad \textbf{[8]}$$

where $I = n^{-1}|\mathbf{E}\times\mathbf{H}^*| = |\mathbf{E_0}|^2$. The factor $\sigma = -2\mathrm{Im}\{(\mathbf{E}\cdot\hat{\mathbf{x}})(\mathbf{E}^*\cdot\hat{\mathbf{y}})\}/(|\mathbf{E}\cdot\hat{\mathbf{x}}|^2 + |\mathbf{E}\cdot\hat{\mathbf{y}}|^2)$ is a measure for the degree of circular polarization (ellipticity) of the wave in the (x, y) plane, such that $\sigma = +1$ for right circular polarization and $\sigma = -1$ for left circular polarization. In the calculations that follow, we will furthermore use the parameters $\tau = (|\mathbf{E}\cdot\hat{\mathbf{x}}|^2 - |\mathbf{E}\cdot\hat{\mathbf{y}}|^2)/(|\mathbf{E}\cdot\hat{\mathbf{x}}|^2 + |\mathbf{E}\cdot\hat{\mathbf{y}}|^2)$ and $\xi = 2\mathrm{Re}\{(\mathbf{E}\cdot\hat{\mathbf{x}})(\mathbf{E}^*\cdot\hat{\mathbf{y}})\}/(|\mathbf{E}\cdot\hat{\mathbf{x}}|^2 + |\mathbf{E}\cdot\hat{\mathbf{y}}|^2)$ as measures for the linear polarization in the (x, y) plane, such that $\tau = \{+1, -1\}$ correspond to linear polarization along $\{x, y\}$ and $\xi = \{+1, -1\}$ correspond to linear polarization at angles of $\{+45°, -45°\}$ with respect to the x axis. The helicity-dependent change of the radiation pressure due to the chiral polarizability χ that shows up in Eq. **8** has previously been used for sorting highly chiral liquid crystal droplets in optical lattices (11). We now may consider an evanescent wave created by the total internal reflection of light at an interface in the (z,y) plane, which has the form $\mathbf{E} = \sqrt{\mu}\mathbf{E_0}\exp(-\kappa x)\exp(ik_z z)$. If the evanescent field is propagating in a medium with index $n_2 = \sqrt{\epsilon\mu}$ and was created through the total internal reflection of a beam in a medium with index n_1 incident on the interface with angle θ in the (x,z) plane (Fig. 1), then the wave vector components are given by $k_z = (n_1/n_2)\sin(\theta)k$, $k_x = \sqrt{k^2 - k_z^2}$, and $\kappa = \sqrt{k_z^2 - k^2} = ik_x$, where $k = n_2\omega/c$. The energy and momentum densities of an evanescent field relevant for the calculation of the forces with Eqs. **2** and **3** are listed in *Supporting Information*. Notably, evanescent fields have longitudinally polarized field components (*Supporting Information*), which give rise to transverse spin angular momentum (17, 31). As mentioned, in case of a p-polarized wave ($\tau = 1$) it is the electric field that is elliptically polarized in the (x,z) plane, and in case of an s-polarized wave ($\tau = -1$) it is the magnetic field. Correspondingly, the out of plane electric and magnetic spin components are given by $(\hat{\mathbf{y}}\cdot\mathbf{s_e}) = (1+\tau)\frac{g}{4\omega}\frac{\kappa}{k_z}I_e$ and $(\hat{\mathbf{y}}\cdot\mathbf{s_m}) = (1-\tau)\frac{g}{4\omega}\frac{\kappa}{k_z}I_e$. Using Eqs. **2**–**6** the forces exerted on a chiral dipole by an evanescent field are given by

$$\mathbf{F_0} = \kappa I_e\left[\mathrm{Re}\{\chi\}n_2\sigma - \frac{1}{2}\left(\mathrm{Re}\{\mu\alpha_e\}\left(1+\tau\frac{\kappa^2}{k_z^2}\right) + \mathrm{Re}\{\epsilon\alpha_m\}\left(1-\tau\frac{\kappa^2}{k_z^2}\right)\right)\right]\hat{\mathbf{x}}$$
$$\frac{I_e}{2}k_z\left[\mathrm{Im}\{\mu\alpha_e\}\left(1+\tau\frac{\kappa^2}{k_z^2}\right) + \mathrm{Im}\{\epsilon\alpha_m\}\left(1-\tau\frac{\kappa^2}{k_z^2}\right) + 2\mathrm{Im}\{\chi\}\sigma n_2\right]\hat{\mathbf{z}} \quad \textbf{[9]}$$

$$\mathbf{F_{int}} = -I_e\frac{k^4}{3}\frac{\kappa}{k_z}\left[\mathrm{Re}\{\alpha_e\alpha_m^*\}\sigma + \mathrm{Im}\{\alpha_e^*\alpha_m\}\xi + \sigma|\chi|^2 + \underbrace{\frac{\epsilon}{n_2}(1-\tau)\mathrm{Re}\{\chi\alpha_m^*\} + \frac{\mu}{n_2}(1+\tau)\mathrm{Re}\{\chi\alpha_e^*\}}_{\text{Chirality–sorting Lateral Force}}\right]\hat{\mathbf{y}}$$
$$-I_e\frac{k^4}{3}\frac{k}{k_z}\left[\mathrm{Re}\{\alpha_e\alpha_m^*\} + |\chi|^2 + \frac{\sigma}{n_2}\left(\epsilon\,\mathrm{Re}\{\chi\alpha_m^*\} + \mu\,\mathrm{Re}\{\chi\alpha_e^*\}\right)\right]\hat{\mathbf{z}}$$
$$-I_e\frac{k^4}{3}\frac{\kappa k}{k_z^2}\left(\frac{\xi}{n_2}\left(\mathrm{Re}\{\mu\chi\alpha_e^*\} - \mathrm{Re}\{\epsilon\chi\alpha_m^*\}\right) + \mathrm{Im}\{\alpha_e^*\alpha_m\}\tau\right)\hat{\mathbf{x}} \quad \textbf{[10]}$$

with $I_e = \frac{|\mathbf{E_0}|^2}{1+\tau(\kappa/k_z)^2}\exp(-2\kappa x)$. The lateral forces experienced by the dipole are due to the $\mathbf{F_{int}}$ term and given by the first line

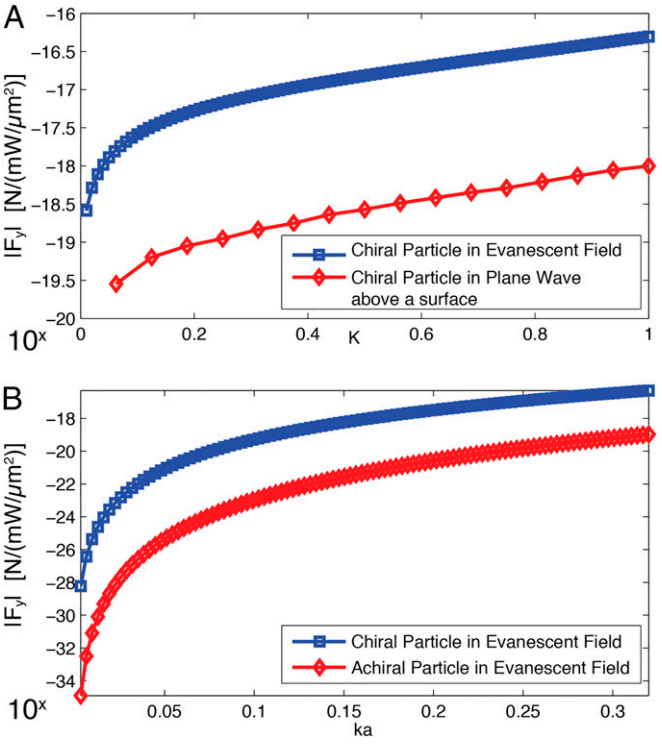

Fig. 2. Lateral optical forces. The previously predicted lateral optical forces in comparison with the lateral force on a chiral particle in an evanescent field. The absolute value of the lateral force F_y is shown on a logarithmic scale in base 10. (*A*) The lateral optical force on a chiral nanosphere in a plane wave above a reflective surface according to Wang and Chan (16) and due to an evanescent field with $\tau = 1$ as a function of the chirality parameter K for positive helicity (20, 33) (*Supporting Information*). The sphere is nonmagnetic, situated 60 nm above the surface, and has a dielectric constant of $\epsilon_s = 2$ and a radius of 30 nm. In case of the force in the evanescent field, the intensity refers to the intensity of a beam that is totally internally reflected at a flint glass/air interface at an angle of $\theta = 36.4°$. (*B*) The lateral force on an achiral sphere ($K = 0$) due to the Belifante spin momentum density according to Bliokh et al. (17) and on an equivalent chiral sphere ($K = 1$) as a function of ka, where a is the radius of the sphere and $k = n_2\omega/c$ is the wavenumber of the evanescent field. In both cases the sphere is nonmagnetic and situated at a height of 30 nm, has dielectric constant $\epsilon_s = 2$, and experiences the evanescent field generated at a flint glass/air interface at an incident angle of $\theta = 36.4°$. In the former case the polarization of the evanescent field has $\sigma = 1$ and in the latter $\tau = 1$.

of Eq. **10**. Adjusting the polarization to $\tau = \pm 1$ renders the lateral forces directly proportional to χ, and their direction is therefore helicity-dependent. Unfortunately, the chirality-dependent lateral forces caused by $\nabla \times \mathbf{p}$ and $\mathbf{s}$ in the $\mathbf{F_0}$ force term exactly cancel each other (32). Small perturbations of the force that may arise due to the reflection of the field scattered by the particle at the interface at which the evanescent field is generated are neglected.

Fig. 2 compares the strength of the force to those of the lateral forces predicted by Wang and Chan (16) and Bliokh et al. (17) as it depends on the chirality and the size of a spherical nanoparticle in an electromagnetic field. In each case, the lateral force emerging through the interaction of the transverse SAM with the chiral particle is stronger by about 1.75 and 4 orders of magnitude over the considered range. Here material chirality is parametrized using the chirality parameter $K = c\chi \in [-1,1]$ assuming real values to mirror what was done in ref. 16. The derivation of the expression of the force on such a sphere is listed in *Supporting Information*, as well as a discussion of the force on helicene molecules and gold nanohelices, which represent other types of chiral particles frequently considered in the literature, and which helps to further illustrate the characteristic magnitude of the force. We furthermore include calculations of the nonlateral force terms acting on these objects.

In summary, we predict lateral forces on materials with chiral optical response in evanescent fields, which push particles with opposite helicities in opposite directions with strength dependent on the chiral polarizability. The forces result from the direct interaction of the evanescent field's transverse optical SAM density of the wave with the chiral electromagnetic response of the particle, and are particularly strong in comparison with previously predicted lateral optical forces. Transverse SAM may arise whenever light is laterally confined, so that the effect described in this paper represents a natural choice for the optical sorting by material chirality in an integrated system. The effect can be produced by a single beam, which avoids standing wave patterns that limit the separation of enantiomers to the width of interference fringes. However, the use of multiple beams may enable the cancellation of the longitudinal force component or, given the possibility of generating transverse spin, even the generation of spin-optical lateral forces in free space beams (34). The fact that the optical spin force described here represents by far the strongest force acting in the lateral direction renders the effect in a sense background-free, which is useful given the generally weak nature of chiral optical effects. Although we limited the discussion to the simplest case of an evanescent field created by the total internal reflection of light at a single interface, there is significant potential for improving the strength of the force by further engineering the light field. Natural choices for this are the intense and inherently evanescent fields of plasmonic excitations, or optical waveguides designed to have regions with high field enhancement, such as slot waveguides (35). We furthermore limited the discussion to the Rayleigh limit, where compact closed-form expressions exist, although the optical manipulation of objects smaller than a few 100 nm in liquid suspension is in general very challenging due to thermal agitation. Other than by tailoring the light fields, this may in particular be overcome in a low-pressure environment, for example in deflecting molecular beams (36). Larger particles may take advantage of resonances (such as Mie resonances) and are bound to experience much stronger forces. An experimental verification of the optical spin force on chiral media is very likely possible using a remarkable recently demonstrated method for measuring lateral optical forces using a cantilever with extremely low compliance (37). By immersing the cantilever into an evanescent field, Antognozzi et al. (37) were able to measure the substantially weaker lateral spin force on achiral materials with femtonewton resolution. In an experiment measuring the force described in this paper, a chiral particle could either be attached to the cantilever, or the cantilever may be manufactured from a chiral material itself (TeO_2 being a standard material).

ACKNOWLEDGMENTS. The authors thank X. Yin for helpful discussions. This research was supported by Air Force Office of Scientific Research Grant FA9550-12-1-0289.

1. Lord Kelvin (1904) *Baltimore Lectures* (C. J. Clay and Sons, London), pp 436, 619.
2. Smith SW (2009) Chiral toxicology: It's the same thing...only different. *Toxicol Sci* 110(1):4–30.
3. Sekhon BS (2009) Chiral pesticides. *J Pest Sci* 34(1):1–12.
4. US Food and Drug Administration (1992) FDA's policy statement for the development of new stereoisomeric drugs. *Chirality* 4(5):338–340.
5. Caner H, Groner E, Levy L, Agranat I (2004) Trends in the development of chiral drugs. *Drug Discov Today* 9(3):105–110.
6. Nguyen LA, He H, Pham-Huy C (2006) Chiral drugs: An overview. *Int J Biomed Sci* 2(2): 85–100.
7. McKendry R, Theoclitou ME, Rayment T, Abell C (1998) Chiral discrimination by chemical force microscopy. *Nature* 391(6667):566–568.
8. Tang Y, Cohen AE (2010) Optical chirality and its interaction with matter. *Phys Rev Lett* 104(16):163901.
9. Tang Y, Cohen AE (2011) Enhanced enantioselectivity in excitation of chiral molecules by superchiral light. *Science* 332(6027):333–336.
10. Canaguier-Durand A, Hutchison JA, Genet C, Ebbesen TW (2013) Mechanical separation of chiral dipoles by chiral light. arXiv:1306.3708.
11. Tkachenko G, Brasselet E (2014) Optofluidic sorting of material chirality by chiral light. *Nat Commun* 5:3577.
12. Tkachenko G, Brasselet E (2014) Helicity-dependent three-dimensional optical trapping of chiral microparticles. *Nat Commun* 5:4491.
13. Cameron RP, Barnett SM, Yao AM (2014) Discriminatory optical force for chiral molecules. *New J Phys* 16(1):013020.
14. Smith D, Woods C, Seddon A, Hoerber H (2014) Photophoretic separation of single-walled carbon nanotubes: A novel approach to selective chiral sorting. *Phys Chem Chem Phys* 16(11):5221–5228.
15. Patterson D, Schnell M, Doyle JM (2013) Enantiomer-specific detection of chiral molecules via microwave spectroscopy. *Nature* 497(7450):475–477.
16. Wang SB, Chan CT (2014) Lateral optical force on chiral particles near a surface. *Nat Commun* 5:3307.
17. Bliokh KY, Bekshaev AY, Nori F (2014) Extraordinary momentum and spin in evanescent waves. *Nat Commun* 5:3300.
18. Bliokh KY, Nori F (2011) Characterizing optical chirality. *Phys Rev A* 83(2):021803.
19. Belinfante FJ (1940) On the current and the density of the electric charge, the energy, the linear momentum and the angular momentum of arbitrary fields. *Physica* 7(5):449–474.
20. Van Mechelen T, Jacob Z (2015) Universal spin-momentum locking of evanescent waves. arXiv:1504.06361.
21. Bliokh KY, Nori F (2015) Transverse and longitudinal angular momenta of light. arXiv: 1504.03113.
22. Nakamura YO (1981) Spin quantum number of surface plasmon. *Solid State Commun* 39(6):763–765.
23. Landau LD, et al. (1984) *Electrodynamics of Continuous Media* (Elsevier, Oxford).
24. Purcell EM, Pennypacker CR (1973) Scattering and absorption of light by nonspherical dielectric grains. *Astrophys J* 186:705–714.
25. Nieto-Vesperinas M, Sáenz JJ, Gómez-Medina R, Chantada L (2010) Optical forces on small magnetodielectric particles. *Opt Express* 18(11):11428–11443.
26. Jaggard DL, Mickelson AR, Papas CH (1979) On electromagnetic waves in chiral media. *Appl Phys* 18(2):211–216.
27. Yin X, Schäferling M, Metzger B, Giessen H (2013) Interpreting chiral nanophotonic spectra: The plasmonic Born-Kuhn model. *Nano Lett* 13(12):6238–6243.
28. Draine BT (1988) The discrete-dipole approximation and its application to interstellar graphite grains. *Astrophys J* 333:848–872.
29. Ho JS, Stell G (1982) Theory of the refractive index of fluids. *J Chem Phys* 77(10):5173–5183.
30. Jackson JD (1962) *Classical Electrodynamics* (Wiley, New York).
31. Bliokh KY, Nori F (2012) Transverse spin of a surface polariton. *Phys Rev A* 85(6): 061801.
32. Bliokh KY, Kivshar YS, Nori F (2014) Magnetoelectric effects in local light-matter interactions. *Phys Rev Lett* 113(3):033601.
33. Lakhtakia A, Varadan VK, Varadan VV (1991) Effective properties of a sparse random distribution of non-interacting small chiral spheres in a chiral host medium. *J Phys D Appl Phys* 24(1). Available at dx.doi.org/10.1088/0022-3727/24/1/001.
34. Bekshaev AY, Bliokh KY, Nori F (2014) Transverse spin and momentum in two-wave interference. arXiv:1407.6786.
35. Yang AH, et al. (2009) Optical manipulation of nanoparticles and biomolecules in sub-wavelength slot waveguides. *Nature* 457(7225):71–75.
36. Sakai H, et al. (1998) Optical deflection of molecules. *Phys Rev A* 57(4):2794.
37. Antognozzi M, et al. (2015) Direct measurement of the extraordinary optical momentum using a nano-cantilever. arXiv:1506.04248.

38. Chaumet PC, Nieto-Vesperinas M (2000) Time-averaged total force on a dipolar sphere in an electromagnetic field. *Opt Lett* 25(15):1065–1067.
39. Barron LD (2004) Molecular *Light Scattering and Optical Activity* (Cambridge Univ Press, Cambridge, UK), 2nd Ed.
40. Gansel JK, et al. (2009) Gold helix photonic metamaterial as broadband circular polarizer. *Science* 325(5947):1513–1515.
41. Gibbs JG, et al. (2014) Nanohelices by shadow growth. *Nanoscale* 6(16):9457–9466.
42. Rogacheva AV, Fedotov VA, Schwanecke AS, Zheludev NI (2006) Giant gyrotropy due to electromagnetic-field coupling in a bilayered chiral structure. *Phys Rev Lett* 97(17):177401.
43. McPeak KM, et al. (2014) Complex chiral colloids and surfaces via high-index off-cut silicon. *Nano Lett* 14(5):2934–2940.